Flow Patterns of Liquids in Agitated Vessels

SHUICHI AIBA

University of Tokyo, Tokyo, Japan

In this paper flow patterns of liquids in an agitated vessel of 11 1/2-in. I.D. were measured with the radioisotope of cobalt as a means of measurement. Flow patterns of representative types of impellers, namely paddle, turbine, and propeller, were studied. Water and glycerine solutions were used as liquids the viscosity of which ranged from 1 to 108 cp. Effects of geometrical factors of agitated systems on flow patterns were investigated, in particular those of baffles.

Experimental results obtained were analyzed, and a curve showing the relation between flow patterns and power consumption by the agitation was made.

Generally agitation in miscellaneous chemical processes is concerned with blending such systems as solid-liquid, liquid-liquid, and liquid-gas with the objectives of increasing mass and heat transfer rates, of increasing physical and chemical reaction rates, of securing homogeneous mixtures, etc.

Many papers on agitation have been published over the past twenty years (*1*); for example, rather detailed information is now available on such problems as how to obtain homogeneous solid suspensions in liquids by using various types of impellers. However it can be seen that this information is not yet comprehensive enough to solve all kinds of problems because agitation itself is complex and because the basic principles have not yet been established. Another reason for this situation is that flow patterns of liquids, which are a fundamental of agitation, yet remain to be studied more thoroughly and quantitatively.

Several years ago the author devised a tiny mechanical instrument to determine flow patterns in an agitated vessel of pilot-plant scale (*2*). Flow patterns were qualitatively measured, and an explanation of the relation between flow patterns and the power requirements of agitation was tentatively made.

Recently Rushton published a paper on flow patterns in an agitated vessel (*4*) in which he measured flow patterns by optical means and determined liquid velocities in the vessel, particularly around the impeller of a flat-blade turbine, photographically. He correlated the pumping capacity of the impeller with these data.

More recently Yamamoto presented a paper on flow patterns and tried to get quantitative analyses from the theory of turbulence also photographically (*5*).

EQUIPMENT AND PROCEDURE

Figure 1 shows the principal parts of the device used to measure flow patterns. A miniature Geiger-Müller (GM) tube of about 25/64 in. in diameter and 1 3/16 in. in length, shielded by an aluminum tube, was hung one one side. On the other side a steel ball of about 11/64-in. diameter, into which an appropriate amount of a radioisotope of cobalt-60 (metal form) was buried, was hung by a platinum wire of 30μ diameter; both elements were immersed.

The intensity of gamma rays was markedly affected by changing the distance between the detector and the radiation source; that is, the intensity of radiation measured by the detector was greatly influenced by the geometrical configurations of the system. The effects of geometrical factors on the measurements of radiation are important in the application of radioisotope techniques.

In the case in which both the detector and the radiation source are immersed in liquids it is difficult to compute the radiation intensity detected by the counter solely on the basis of the geometrical configurations of the system because the multiple scattering phenomenon becomes predominant.

However in the special case in which the distance between the elements is not too large and the radiation source is located centrally along the length of the GM tube, the interrelation between the radiation intensity N_0 counts/min. and the distance could be calibrated, as shown in Figure 2.

When one uses such a calibration curve, the measurement of N_0 leads to the determination of l rather easily and accurately when the latter is unknown. When the liquid is in motion, the radiation source P is transpositioned to P' as a result of the balance of moment around A with liquid velocity head (Figure 3). Then the following equation of balance is obtained, in which the resistance of the platinum wire is negli-

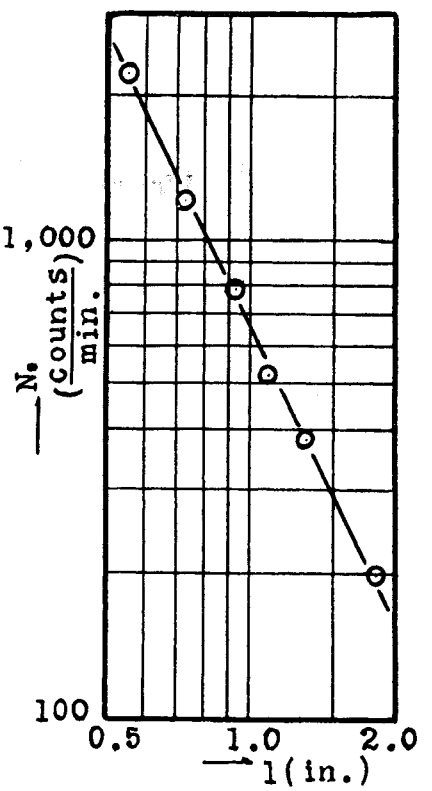

Fig. 2. Example of calibration curve.

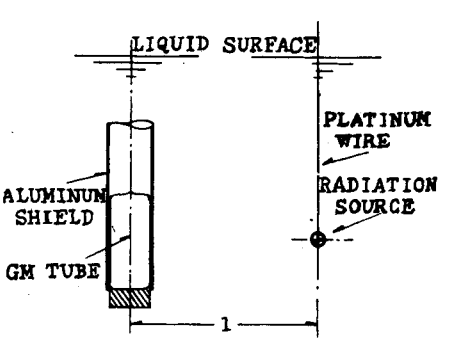

Fig. 1. Principal part of a device to measure flow velocity.

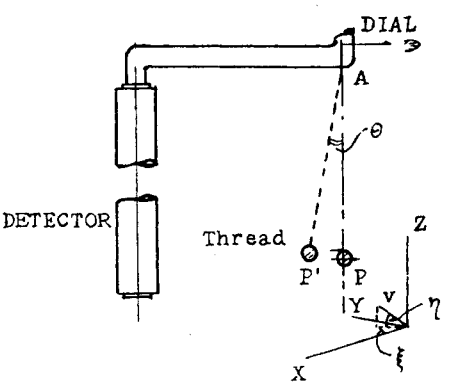

Fig. 3. Balance of moment with liquid velocity.

Table 1. Representative Dimensions of Impellers Used

	L, in.	W, in.	Number of blades
Paddle	4 46/64	5/8	2
Flat blade turbine (4)	3 15/16	25/32	6
Marine propeller	2 61/64	19/32*	3

*Mean along the radius.

Table 2. An Example of Calculated Results

ω	C**	C*	Re*
7.35	3.93	12.6	1.47×10^4
10.2	3.28	10.6	2.08×10^4
12.5	3.07	9.90	2.50×10^4
15.7	2.96	9.50	3.13×10^4
21.0	2.60	8.35	4.20×10^4

Paddle (L = 4-46/64, W = 5/8 in., unbaffled. liquid, water).

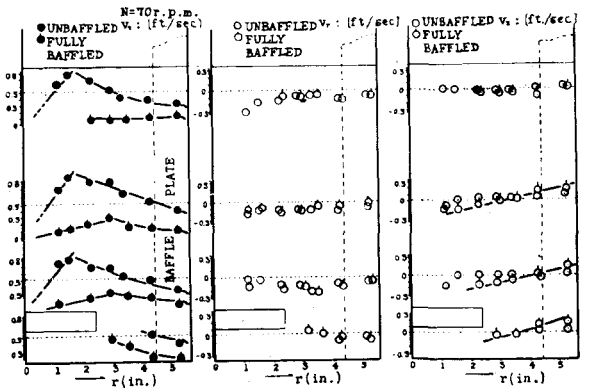

Fig. 4. Example of flow patterns (water)
N = 70 rev./min. (unbaffled and fully baffled paddle) surface at which flow velocity was measured.

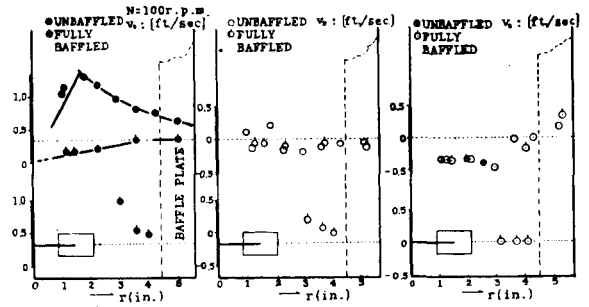

Fig. 5. Example of flow patterns (water)
N = 100 rev./min. (unbaffled and fully baffled turbine).

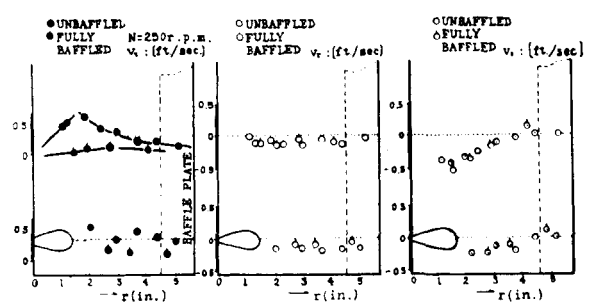

Fig. 6. Example of flow patterns (water)
N = 250 rev./min. (unbaffled and fully baffled propeller).

gible, compared with that of the steel ball.

$$\left(\frac{\pi}{6}\right)\cdot D_P^3\cdot(\rho_s - \rho)g\cdot\sin\theta = C\left(\frac{\rho}{2}\right)\cdot v^2\cdot\left(\frac{\pi}{4}\right)\cdot D_P^2\cdot\cos(\theta \mp \eta) \qquad (1)$$

The term sin θ in Equation (1) was calculated from the transposition of the ball from P to P' by determining the radiation intensity N_0 in such a way that the axis of the GM tube was vertical and lay in the same plane as point A and the radiation source P' (Figure 3).

Moreover, by measuring η in Equation (1) through a procedure which will be described later, the following equation was obtained relating to each experimental condition:

$$C\cdot v^2 = \text{const.} \qquad (2)$$

For each experimental determination all factors on the right-hand side of Equation (2) were known, and for this determination this side is a constant.

The liquid velocity v at each point in the vessel was easily determined by trial and error from this equation, with the help of the drag-coefficient data of the ball. The liquid velocity thus obtained is considered to be the average for the period of time of each experiment.

A cylindrical glass vessel about 11½ in. in diameter and 14 in. high was used as the agitation vessel throughout this series of experiments. Glycerine and water were used as liquids. In most cases the vessel was filled to the depth of 11 in. Three representative types of impeller, that is, paddle, turbine, and marine propeller, were used. Each impeller was placed concentrically about 1 13/64 in. above the bottom of the vessel. Representative dimensions of these impellers are shown in Table 1. In each case flow patterns were measured under unbaffled and fully baffled* conditions. Four baffle plates, each 1 13/64 and 12 in. in width and length, respectively, were attached to a cage, which could be removed from the vessel for unbaffled operation.

To measure liquid velocity the device shown in Figure 3 was fixed at a certain radial position for each depth under the liquid surface. Varying the location of the device determined flow patterns throughout the vessel except in the immediate vicinity of each impeller.

Under fully baffled conditions, with the expectation that the velocity distribution might be changed depending on the radial direction along which the measuring instrument was fixed, experiments were made to determine the velocity distribution along several radial directions between the baffle plates. No difference was apparent among them. Then experiments were made, under fully baffled conditions, exclusively along the radius just midway between two baffle plates. This excludes of course the situation immediately behind or in front of each baffle plate, which cannot be studied by the instrument. For unbaffled conditions the effect was assumed to be negligible because of the symmetry of the flow, radially as well as peripherally.

When one compares the dimension of this device with the dimensions of the vessel, the effect of disturbances caused by the device on the flow patterns was assumed to be negligible, as far as this series of experiments was concerned. In Equation (1) η was determined as follows: The vertical distance between the tip of a tiny string (1 13/64 in. long) attached to the ball and an imaginary horizontal line drawn through the center of the ball was measured by a cathetometer from outside the vessel.

The angle ξ subtended by the xy projection of the velocity vector and the x axis was measured during the determination of sin θ with the help of a dial placed horizontally around the shaft (Figure 3). In this case the radial direction was arbitrarily chosen as the y axis.

When the determination of low velocity was necessary, an acryl-resin ball of about 7/64-in. diameter, containing an appropriate amount of cobalt-60, was used as the radiation source. It was determined by preliminary experiments that the flow resistance of the platinum wire which suspended the ball was not an appreciable source of error. It was also determined that

Fully baffled conventionally means that the peripheral flow is completely impeded by a certain number of baffle plates causing vertical flow components. Usually four baffle plates are used.

the wire did not bend, owing to the liquid flow.

Constant precautions were taken to assure the calibration stability of the miniature GM tube, and a calibration curve as shown in Figure 2 was prepared before each experiment to check the reliability of the whole circuit, including the GM tube. It was estimated that the experimental error inherent in the circuit was about 2 to 3%.

Simple geometrical corrections were made concerning the position at which the liquid velocity was measured because of the transposition of the ball from P to P'. Liquid velocity thus measured was resolved into vectors v_t, v_r, and v_z for ease of comparing experimental results.

Along with the flow pattern determinations the power consumption of the agitators was also measured. The dynamometer used was a spring type, the deflections of which were transmitted by a pair of self-synchronous motors. Judging from the modified Reynolds number, one sees that this series of experiments was made covering the turbulent region as well as the transition region from turbulent to laminar flow.

EXPERIMENTAL RESULTS

Flow Patterns of Representative Types of Impellers

The Case of Unbaffled Operations (Water)

Flow patterns of a paddle, a turbine, and a propeller are shown in Figures 4, 5, and 6, respectively, when water was used as the liquid. In each figure data obtained under unbaffled and fully baffled conditions are superimposed for ease of comparison. Peripheral, radial, and vertical components are shown individually from left to right in these figures. The abscissa of each figure represents the distance from the center of the vessel.

The liquid level at a standstill is shown in Figure 4. (See also Figures 7 and 8.) Though the level is not clear in Figures 5 and 6, it was described before (11 in.). Moreover, since the velocity is independent of the depth within the tank, as is apparent in Figure 4, the determination of the velocity was simplified in Figures 5 and 6. The data points show the actual elevations. The dotted lines indicate the depth to which the measuring instrument was immersed in each experiment.

When one refers to these figures, the following facts seem to be apparent. In the case of unbaffled agitation, irrespective of the type of impeller, two flow regions existed in the vessel relating to the peripheral velocity component. In the region found around the center of the vessel the liquid seemed to rotate as a whole, as if it were a solid (cylindrical forced vortex). In the other region, found between the former and the vessel wall, the liquid rotated along with the cylindrical vortex (free vortex).

When many experimental results other than those shown in Figures 4, 5, and 6 were reviewed, it was found that the radius of the cylindrical vortex was constant, irrespective of the rotational speed of the impeller as well as of its location inside the vessel. It is presumed that r_F is influenced mainly by the geometrical conditions of the agitation system and the physical properties of the liquid, in particular by the viscosity. The latter effect will be described later.

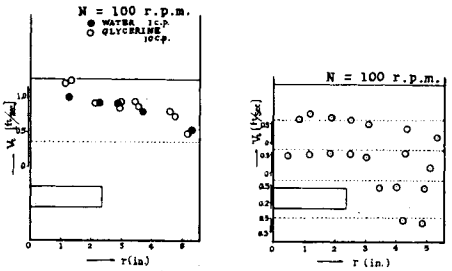

Fig. 7. Flow patterns of glycerine solution (unbaffled paddle).

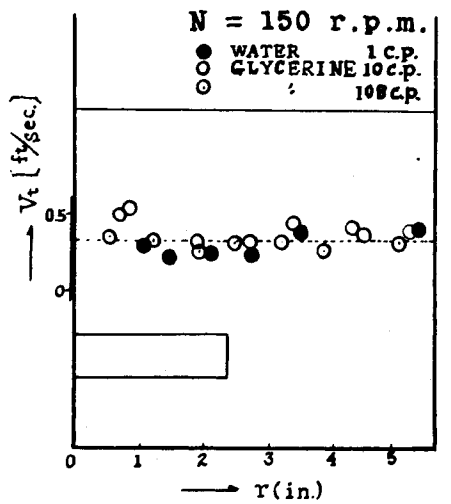

Fig. 8. Flow patterns of glycerine solution (fully baffled paddle).

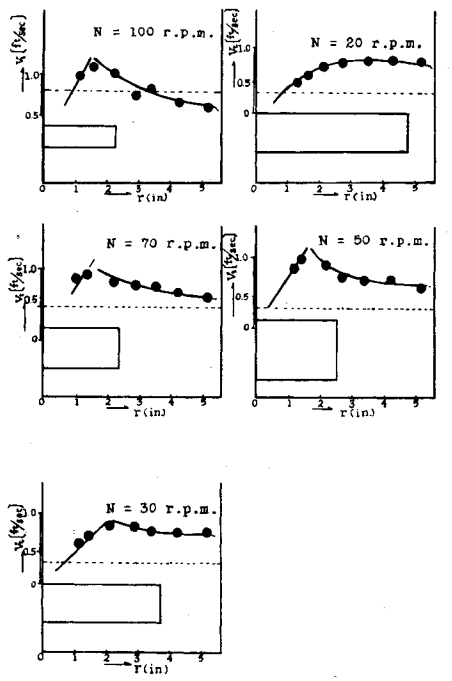

Fig. 9. Effect of geometrical dissimilarity (unbaffled paddle, liquid: water).

Outside the cylindrical vortex, tangential velocity was experimentally found to be

$$v_t = C_5 r^{-n_0} \qquad (3)$$

Inspection of many experimental results shows that

$$n_0 = 1 \sim 0$$

Furthermore, it was found that n_0 approached unity as the location of the velocity measurement approached the liquid surface; therefore liquid velocity becomes more averaged owing to fluctuations or turbulence in the vicinity of each impeller. In the case of the paddle, in particular, it was found that radial as well as vertical velocity components were nearly independent of r except for the region adjacent to the impeller.

When one considers the radial component, the negative direction is that toward the tank center. In each figure the positive direction is not always apparent; however the positive direction of flow, namely, the radial flow toward the tank wall, should exist, as may be deduced from the simple concept of a material balance. It is assumed that such flows might exist in the region just adjacent to the impeller or to the tank wall when the positive direction is not apparent. Study of such a region is beyond the scope of this investigation.

The small-scale circulation, radially or vertically, could not be determined, owing to the geometry of the measuring instrument. If stress is placed on such details, other appropriate procedure should be adopted, say for example, optical means. Moreover the data obtained experimentally are not refined enough to define local swirls or small eddies. The fact that positive radial flow vectors or reasonable vertical components could not be found because of the difficulty of their determination does not indicate that the data which were obtained are in error. In the case of turbine and propeller types of impellers radial discharge and suction flow were more apparent, even in the case of unbaffled condition. Generally it can be seen that the flow patterns of the paddle, turbine, and propeller types of impellers are characterized by peripheral, radial, and axial flows, respectively, when unbaffled conditions are in effect.

The Case of Fully Baffled Operation

In the case of fully baffled operation the flow pattern is characterized by a marked decrease in the tangential velocity component, irrespective of the impeller type. The radial component remains almost unchanged. Moreover the tangential velocity decreased as the location at which the velocity was measured approached the liquid surface (Figure 4). For each impeller, when one refers to the

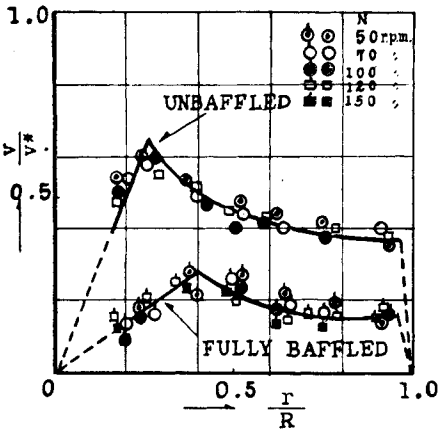

Fig. 10. Review on flow patterns (paddle).

other figures obtained, there were certain cases in which the so-called "cylindrical" vortex was found rather distinctly. However the radius of the cylindrical vortex was larger than that observed in the case of unbaffled condition. Even in the case of paddle type of impellers, upward and downward flow became apparent.

Effect of Viscosity

The effect of liquid viscosity on flow patterns is shown in the case of the paddle type of impeller for unbaffled and fully baffled conditions in Figures 7 and 8, respectively. In these figures only the tangential velocity component is shown. From Figure 7 it is to be noted that tangential velocity does not decrease markedly along liquid depth even in the case of the viscous liquid (viscosity = 108 centipoises). In the unbaffled case, as liquid viscosity increased, the boundary between forced and free vortex became more vague, and the region of forced cylindrical vortex became narrowed down around the center of the vessel. Such a tendency can also be seen in the case of fully baffled conditions. However it is seen that the difference of flow patterns relating to unbaffled and fully baffled conditions is not so great as that noted when water was used. The effect of liquid viscosity will be considered again in the discussion of experimental results.

Effect of Impeller Geometry

Since the effect of geometry on flow patterns can be most distinctly seen in the tangential velocity component for each impeller under unbaffled conditions, experimental data for the paddle type of impeller, with water used as the liquid, are presented in Figure 9 as an example. Figure 9 is based upon the total tangential velocity gradient along the radius. Different speeds were chosen mainly for convenience in experimenting. However, by referring to Figure 10, which will be described later (unbaffled case, tangential velocity predominant), one can see that the flow pattern under any revolutional speed is represented by

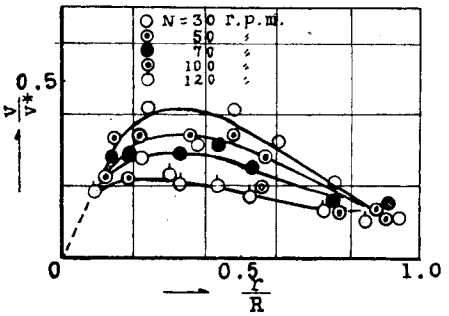

Fig. 11. Review on flow patterns (unbaffled paddle, glycerine solution 108 centipoises).

the gradient of tangential velocity. It is to be noted from these figures that impeller span is more effective than width in decreasing the velocity gradient in the free vortex region.

DISCUSSION OF EXPERIMENTAL RESULTS

Summary of Flow-Pattern Behavior

In this summary the data for paddle type of impellers for the case in which water was used as liquid are considered, based on many data other than those shown in Figure 4; Figure 10 shows the results. In this figure the ordinate is the ratio of the liquid velocity at a given depth from the liquid surface (in this case about 7 in.) to the tip velocity of the impeller. The abscissa is the ratio of the distance from the vessel center at which the velocity was measured to the vessel radius. In Figure 10 parameters are the rotational speeds of the impeller. It is seen that the flow patterns are independent of N. This fact is significant because it constitutes one of the clues with which to judge whether or not the flow is turbulent. If v/v_L were to be used as the ordinate in Figure 10, the flow patterns which are independent of N and dependent of r/R would be obtained. In the so-called "turbulent" region the same fact was found experimentally for other types of impellers also.

Figure 11 shows the effect of liquid viscosity. It can be seen from this figure

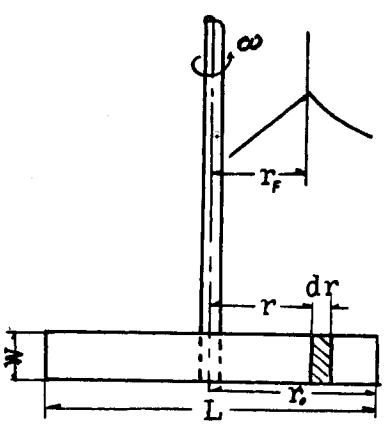

Fig. 12. Schematic diagram of the relation between flow pattern and power consumption of agitation.

that liquid viscosity has a significant influence on the flow patterns as indicated by increased slip between the liquid and the impeller surface as the impeller speed increases. Thus the effect of viscosity is not negligible, as would be suspected from a consideration of the Reynolds number.

The Correlation Between Flow Patterns and Power Consumption

For simplicity the correlation between flow patterns and power consumption will be considered first for the case of the paddle type of impeller. Schematically the flow pattern relating in particular to tangential velocity components is drawn in Figure 12.

It is assumed that liquid viscosity is negligible, as far as flow patterns in the turbulent region and in the steady state are concerned. It is further assumed that Helmholtz's theory of conservation of vorticity is applicable to the vortex tube which was found experimentally to exist in the vessel. This tube is assumed to extend from the liquid surface to the vessel bottom, just encompassing the impeller. The vorticity of a cross section of this tube is $2\omega_0$, and its circulation is $2\pi r_F^2\omega_0$. Vorticity around the impeller is assumed to be $2\pi r_0^2\omega'$.

$$\omega' = \left(\frac{r_F}{r_0}\right)^2 \cdot \omega_0 \tag{4}$$

The torque with length, width, and angular velocity of L, W, and ω, respectively, is calculated by the following equation:

$$T = \int dT = \int C' \frac{\rho(v_i - v_t)^2}{2g_c} \cdot W \cdot r \cdot dr \tag{5}$$

$$\left.\begin{aligned} v_L &= r\cdot\omega \\ v_t &= r\cdot\omega' \\ W/r_0 &= \alpha \end{aligned}\right\} \tag{6}$$

When one substitutes Equation (6) into Equation (5) and postulates C^* as an average of C' covering the integration range from $r = 0$ to $r = r_0$,

$$T = \frac{C^*\cdot\rho\cdot\alpha\cdot r_0(\omega - \omega')^2}{2g_c} \int_{r=0}^{r=r_0} r^3\, dr$$

$$= \frac{C^*\cdot\rho\cdot\alpha\cdot(\omega - \omega')^2}{8g_c} \cdot r_0^5 \tag{7}$$

The power consumption of agitation becomes

$$P_0 = T\cdot\omega = \frac{C^*\cdot\rho\cdot\alpha\cdot\omega\cdot(\omega-\omega')^2}{8g_c} \cdot r_0^5$$

$$= \frac{C^*\cdot\rho\cdot\alpha\cdot\omega\cdot(\omega-\omega')^2}{(8)(32)g_c} \cdot L^5 \tag{8}$$

Also

$$C^*\cdot\omega\cdot(\omega - \omega')^2 = C^{**}\cdot\omega^3 \tag{9}$$

By introducing C^{**} defined by Equation

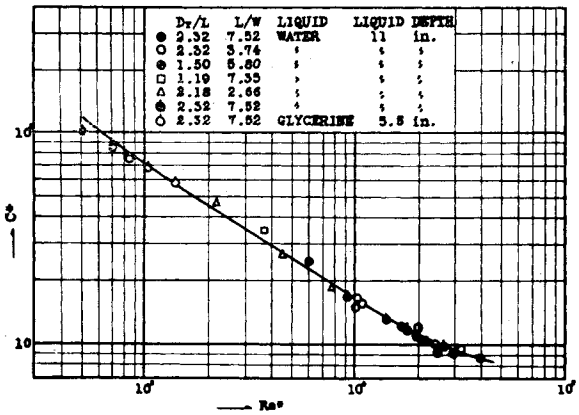

Fig. 13. Correlation between C^* and Re^*.

(9), Equation (10) is obtained from Equations (8) and (9).

$$P_0 = \frac{C^{**} \cdot \rho \cdot \alpha \cdot \omega^3 \cdot L^5}{(8)(32) g_c} = \frac{C^{**} \cdot \rho \cdot \alpha \cdot (2\pi n)^3 \cdot L^5}{(8)(32) g_c} = \frac{C^{**} \cdot \rho \cdot \alpha' \cdot n^3 \cdot L^5}{g_c} \qquad (10)$$

And

$$\alpha' = \frac{(2\pi)^3 \cdot \alpha}{(8)(32)} = (0.966) \cdot \alpha \qquad (10a)$$

Accordingly the power number is

$$N_P = \frac{P_0 \cdot g_c}{n^3 L^5 \rho} = \alpha' \cdot C^{**} \qquad (11)$$

For the region around the impeller, from which the energy required for agitation disseminates into liquid, Equations (9) and (11) show the interrelation between flow patterns and power consumption of agitation. Using the data for power consumption for a given geometrical agitation system, one can calculate C^{**} from Equation (10). From flow-pattern measurements numerical values of (r_F, ω_0) can be found. Then the relative angular velocity of liquid on the surface of the impeller may be estimated from Equation (4), followed by the determination of C^* from Equation (9). For example, for a paddle type of impeller (L = 4 46/64 in., W = 5/8 in., liquid: water) calculated results are shown in Table 2, in which Re^* is defined as

$$Re^* = \frac{r_0^2 \cdot \omega \cdot (1 - \omega'/\omega) \cdot \rho}{\mu}$$

Such calculations, based on data for flow patterns as well as power determinations, were made for other paddles of various dimensions, both unbaffled and fully baffled. The results are shown in Figure 13.

It is noted from this figure that, in spite of a rather wide range of experimental conditions and irrespective of baffled and unbaffled conditions, the relation between Re^* and C^* is rather simple. For the other types of impellers, in particular flat blade turbines, correlation curves which coincide with that of Figure 13 were obtained by similar calculations (*3*). For propeller type of impellers, in which drag due to lift cannot be neglected, a similar relation was found by introducing a correction factor which is a function of the drag coefficient, lift coefficient, and the angle between the blade and the plane of rotation (*3*).

It is to be noted that local velocity information, in particular the radius of the forced-vortex region within the tank, is necessary for the prediction of power consumption by use of Figure 13.

CONCLUSIONS

1. A means of measuring flow patterns in an agitation vessel was devised by applying radioisotope techniques.
2. Flow patterns of representative types of impellers, namely paddles, turbines, and propellers, were measured by this procedure.
3. Effects of geometrical factors on flow patterns were investigated. In particular, effects of baffle plates on flow patterns were studied.
4. It was found that flow patterns for a given agitation system are independent of the impeller speed in the turbulent region. This does not hold true for the case of viscous liquids, when agitation is far from turbulent.
5. Based on several assumptions, a correlation between flow patterns and power consumption was made. A rather simple and unique curve was obtained between Re^* and C^*, covering the whole range of this experimentation.

ACKNOWLEDGMENT

The author wishes to express his cordial thanks to Professor Y. Ohyama of the Tokyo Institute of Technology for his constant guidance throughout this work. He is also indebted to Professor J. L. York of the University of Michigan for his encouragement to publish this paper.

NOTATION

C_0 = experimental constant
C = drag coefficient of ball
C' = drag coefficient
C^* = drag coefficient of impeller
C^{**} = drag coefficient of impeller
D_P = ball diameter, in., ft.
D_T = vessel diameter, in., ft.
g = acceleration due to gravity, ft./sec.^{2}
g_c = conversion factor, (lb.-mass)(ft.)/(lb.-wt.)(sec.^{2})
l = distance between the radiation source and the detector, in.
L = impeller diameter, in., ft.
n = revolutional speed of impeller, rev./sec.
N = revolutional speed of impeller, rev./min.
N_0 = number of gamma quantum per unit time detected by the GM counter
N_P = power number
P_0 = power consumption of agitation, (lb.-wt.)(ft.)
r = distance from the vessel center, in., ft.
r_0 = half of impeller length, in., ft.
r_F = radius of a cylindrical vortex which rotates as if it were solid, in.
R = vessel radius, in.
Re = Reynolds number, ft. of impeller
T = torque imposed on impeller, (lb.-wt.)(ft.)/sec.
v = liquid velocity ft./sec.
v^* = tip velocity of impeller, ft./sec.
v_L = tangential velocity of a point on the impeller, ft./sec.
v_t = tangential velocity component, ft./sec.
v_r = radial velocity component, ft./sec.
v_z = vertical velocity component, ft./sec.
W = impeller width, in., ft.

Greek Letters

ρ = liquid density, lb./cu. ft.
ρ_s = ball density, lb./cu. ft.
μ = liquid viscosity, lb./(ft.)(sec.)
ω_0 = half of vorticity, radian/sec.
ω = angular velocity of impeller, radian/sec.
ω' = angular velocity of liquid on the surface of impeller, radian/sec.

LITERATURE CITED

1. Aiba, Shuichi, *Chem. Eng. (Japan)*, **15**, 354 (1951).
2. ———, *J. Sci. Research Inst., Tokyo*, No. 1286 (1952).
3. ———, *Chem. Eng. Japan*, **20**, 290, 298, 571 (1956).
4. Rushton, J. H., *Chem. Eng. Progr.*, **50**, 597 (1954).
5. Yamamoto, Kazuo, *Chem. Eng. Japan*, **20**, 685 (1956).

Manuscript received October 21, 1957; revision received December 19, 1957; paper accepted May 19, 1958.